eISSN: 3031-9471 | pISSN: 3032-7245 | DOI: 10.69606/geography.v3i3.291

Pubsains Journal of Geographical Sciences and Education

https://journal.pubsains.com/index.php/jgs

[Research Article]

Check for updates

Analysis of Land Cover Change in Relation to the Urban Heat Island Phenomenon using Remote Sensing and GIS Technology in South Jakarta, Indonesia

Ella Whidayanti*, Muhammad Syauqi Labib, Nabilah Rizki Novani, Syahla Nuzla Hazani, Muhammad Akyas

Department of Geography, Faculty of Mathematics and Natural Sciences, Universitas Indonesia

Correspondance: ella.whidayanti@ui.ac.id

Article Info:

Received:
21 July 2025

Accepted:
23 August 2025

Published:
1 September 2025

Keywords:
urban heat island; land cover; NDVI; NDWI; NDBI; remote sensing.

Abstract

The Urban Heat Island (UHI) phenomenon is one of the most significant environmental impacts resulting from land cover changes in urban areas. This study aims to analyze the relationship between land cover change and the UHI phenomenon in South Jakarta through the use of remote sensing and Geographic Information System (GIS) technologies. The data used comprise Landsat-8 OLI/TIRS from 2015 to 2018 to generate NDVI, NDWI, NDBI, Land Cover, and Land Surface Temperature (LST) indices. Pearson correlation test was also conducted to determine the variables that most influence the UHI phenomenon. The land cover changes, particularly the expansion of built-up areas and the reduction of vegetation—directly contribute to an increase in surface temperature. The correlation analysis reveals that NDBI consistently exerts the strongest influence on UHI (0.55), followed by NDWI (0.21) and NDVI (0.18). This research underscores the critical importance of land-use regulation as a strategic approach to mitigating UHI in urban environments.

Informasi Artikel:

Diterima:
21 Juli 2025

Disetujui:
23 Agustus 2025

Dipublikasi:
1 September 2025

Kata kunci:
urban heat island; tutupan lahan; NDVI; NDWI; NDBI; penginderaan jauh.

Abstrak

Fenomena Urban Heat Island (UHI) merupakan salah satu dampak lingkungan yang signifikan akibat perubahan tutupan lahan di kawasan perkotaan. Penelitian ini bertujuan untuk menganalisis hubungan antara perubahan tutupan lahan dengan fenomena UHI di Jakarta Selatan melalui penerapan teknologi penginderaan jauh dan Sistem Informasi Geografis (SIG). Data yang digunakan meliputi citra satelit Landsat-8 OLI/TIRS tahun 2015 hingga 2018 untuk menghasilkan indeks NDVI, NDWI, NDBI, Land cover, dan Land Surface Temperature (LST). Uji korelasi Pearson juga dilakukan untuk menentukan variabel yang paling berpengaruh terhadap fenomena UHI. Perubahan tutupan lahan, terutama peningkatan area terbangun dan penurunan vegetasi, berkontribusi langsung terhadap peningkatan suhu permukaan. Uji korelasi menunjukkan bahwa NDBI merupakan variabel yang paling berpengaruh secara konsisten terhadap UHI (0,55), kemudian NDWI (0,21) dan NDVI (0,18). Penelitian ini menegaskan pentingnya pengendalian perubahan tata guna lahan sebagai strategi mitigasi UHI di kawasan perkotaan.

INTRODUCTION

The Urban Heat Island (UHI) phenomenon refers to the condition in which urban areas exhibit significantly higher surface and air temperatures compared to their surrounding rural regions (Deilami et al., 2018). Urban heat island is primarily a manifestation of increased surface temperatures driven by urbanization activities, particularly land cover changes involving the conversion of vegetated areas into built-up land. The distribution of heat in urban environments is spatially heterogeneous and is strongly influenced by factors such as building density, vegetation cover, the presence of water bodies, and surface characteristics (Weng, 2001). The rise in temperature associated with UHI not only compromises urban thermal comfort but also poses negative impacts on environmental quality and public health (Imhoff et al., 2010).

The rapid rate of urbanization in major cities, including Jakarta, has led to a significant increase in physical development and anthropogenic activities, which in turn have affected environmental temperatures. As one of the most dynamically developing administrative regions, South Jakarta has experienced substantial growth in the residential, industrial, and service sectors, accompanied by a decline in the extent of green open spaces (GOS). According to data from Statistics Indonesia (BPS) for Special Capital Region Jakarta, the population of South Jakarta reached approximately 2.36 million in 2024. This figure reflects a steady upward trend since 2019, with a compound annual growth rate of approx-imately 0.082% over the past five years. The increase in population is directly proportional to the growing demand for land, which has triggered a large-scale conversion of vegetated areas into built-up land (Danniswari et al., 2020).

Land cover conversion is a primary driver of the UHI phenomenon. Previous studies have demonstrated that changes in land cover, particularly the transformation of vegetated areas into residential or industrial zone have a direct impact on increasing surface temperatures (Zhou et al., 2016). Human activities in urban areas, especially in zones characterized by high building density and a lack of GOS, contribute to anthropogenic heat emissions that exacerbate the effects of UHI (Santamouris, 2015). Although the UHI phenomenon in South Jakarta is notably significant, an analysis using the Temperature and Humidity Index (THI) indicates that, with a THI value of 9.7% the region still maintains a relatively higher level of thermal comfort compared to other areas in the Special Capital Region of Jakarta (Wati & Fatkhuroyan, 2017).

Given the intricate interactions among land conversion, building density, vegetation cover, and water bodies, an analytical approach is required to comprehensively depict the UHI phenomenon in South Jakarta. Conventional field-based monitoring methods often face spatial and temporal limitations, making them less effective in representing the dynamics of land-use change and its thermal implications. Therefore, the application of remote sensing and satellite imagery-based mapping offers a more efficient alternative for identifying land cover changes and their relationship with surface temperature variations in urban environments.

The application of remote sensing and Geographic Information System (GIS) technologies facilitates the mapping and spatial analysis of the UHI phenomenon. The primary indicators employed in this study are Land Surface Temperature (LST), Normalized Difference Vegetation Index (NDVI), Normalized Difference Water Index (NDWI), and Normalized Difference Built-Up Index (NDBI). In the analysis of UHI, LST serves as a direct indicator of surface temperature, NDVI evaluates the contribution of vegetation in mitigating heat through evapotranspiration, NDWI measures moisture availability that influences thermal stability, and NDBI reflects the density of built-up areas, which is strongly correlated with anthropogenic heat accumulation. These four indicators can be extracted from satellite imagery, including Landsat, Sentinel, and MODIS data (Weng et al., 2004), which have been utilized since 1972 and have progressively advanced with innovations in image classification techniques, radiometric correction, and multitemporal integration (Schwarz et al., 2011). These methods enable spatial and temporal monitoring of temperature and land cover changes with high accuracy and improved efficiency.

The study of the UHI phenomenon in South Jakarta is highly relevant, as this area is experiencing rapid physical growth and holds a strategic role as a center of residential, economic, and public service activities in Special Capital Region of Jakarta. The environmental pressures

generated in this region differ significantly from those in other areas, thereby necessitating a more detailed understanding of UHI dynamics within this specific urban context.

In line with the dynamics of urban development and the high intensity of the UHI phenomenon in South Jakarta, this study aims to analyze land cover changes and their relationship with UHI phenomenon through the utilization of LST and associated indices (NDVI, NDWI, NDBI) using remote sensing technology. The results of this research are expected to contribute to the formulation of spatially based UHI mitigation strategies, thereby supporting adaptive and sustainable urban spatial planning.

METHOD

This study was conducted in the Administrative City of South Jakarta, one of the municipalities within the Special Capital Region of Jakarta, Indonesia (Figure 1). Geographically, South Jakarta is located between 106°22′42″ - 106°58′18″E and 5°19′12″S, encompassing an area of approximately 145.37 km^2, which accounts for about 22.41% of the total area of Special Capital Region Jakarta Province. This area holds a strategic role in the urban structure of Jakarta as it serves as a link between the capital's economic activity centers and the greater Greater Jakarta metropolitan agglomeration. This strategic position is further supported by the development of transportation infrastructure, such as arterial roads, toll roads, and mass rapid transit/bus rapid transit systems, which facilitate such connectivity (Winarso et al., 2015).

Physiographically, South Jakarta is classified as a lowland area with an average elevation of approximately 26.2 m.a.s.l and a slope gradient of <0.25%. However, the southern part of this region features undulating topography, particularly in areas further away from the flood control canals (Danniswari et al., 2020). South Jakarta is one of the most densely populated urban areas, predominantly composed of residential zones interspersed with urban-scale commercial centers. These characteristics make the area highly relevant for spatial studies on land cover and the UHI phenomenon, as it integrates socio-economic factors, spatial planning, and intensive land use dynamics (Zhou et al., 2014).

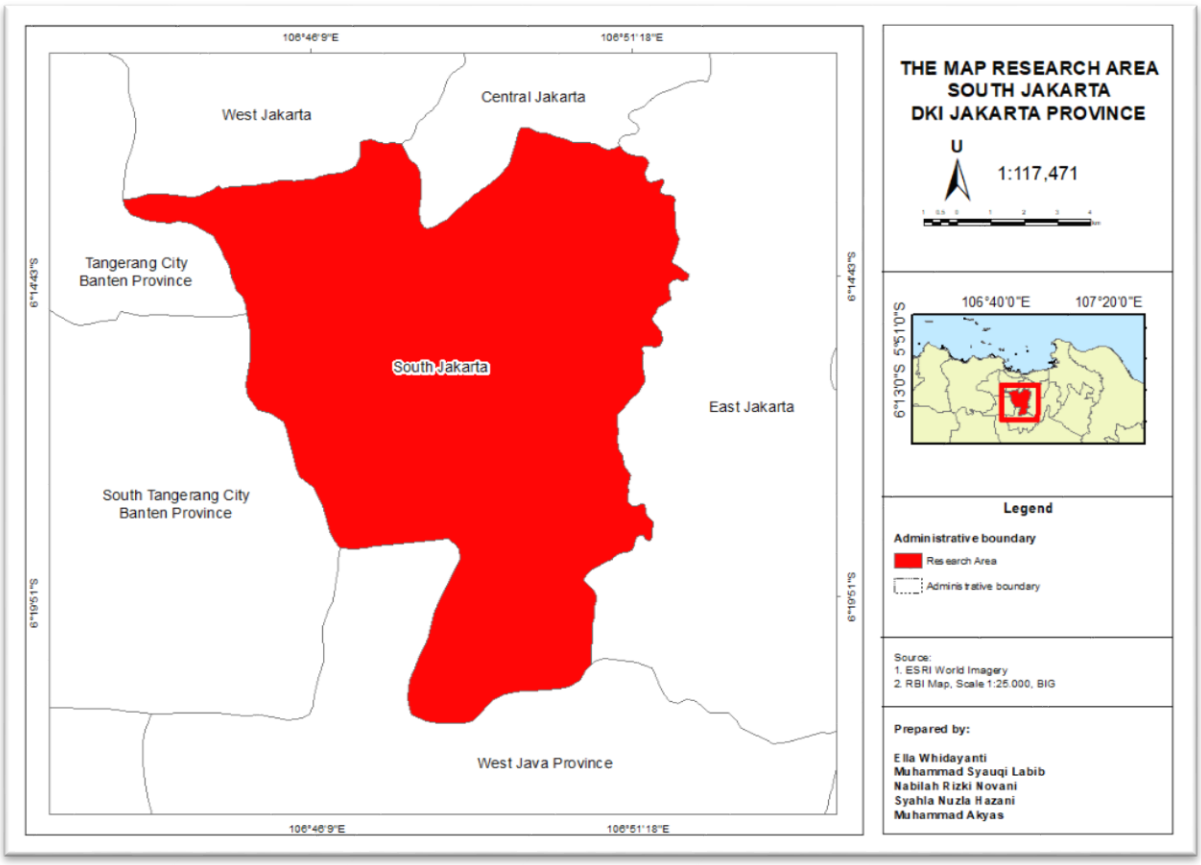

Figure 1. The Map Research Area of South Jakarta

The variable used this study include the NDVI, NDWI, NDBI, land cover, and LST. The NDVI, NDWI, NDBI, land cover, and LST data were derived from the processing of Landsat 8 OLI/TIRS imagery for the years 2015, 2016, 2017, and 2018 using ArcGIS 10.8. This study employed the Pearson Product-Moment statistical test to analyze the correlation between variables. The test was used to quantitatively measure the degree of correlation between two variables on an interval scale. The classification of Pearson's correlation coefficient (*r*) values is presented in Table 1.

Table 1. Pearson's correlation coefficient classification

Coefficient Interval	Degree of Correlation
0.80 – 1.00	Very strong
0.60 – 0.79	Strong
0.40 – 0.59	Moderate
0.20 – 0.39	Weak
0.00 – 0.19	Very weak

Source: Mukaka, 2012.

Data Processing

Normalized Difference Vegetation Index

Vegetation index processing in this study employed the NDVI, which compares the ratio between band 4 (Near-Infrared/NIR) and band 3 (Red) (Whidayanti et al., 2021). The wavelengths of band 4 (0.76-0.90 μm) and band 3 (0.63-0.69 μm) exhibit significant reflectance contrast between vegetation and bare soil surface, making NDVI effective in detecting vegetation density levels (Eastman, 1997; USGS, 2023). The Equation 1 used to calculate NDVI is as follows.

$$NDVI = \frac{(NIR - Red)}{(NIR + Red)} \quad (1)$$

where NIR represents the reflectance of near-infrared light, and Red represents the reflectance of red light. Subsequently, the calculated index values were classified into vegetation density classes (Table 2).

Table 2. Classification of NDVI Values Based on Vegetation Density

NDVI Values (μm)	Density Classification
0.006 – 0.328	Rare
0.335 – 0.427	Medium
0.434 – 0.750	Dense

Source: Department of Forestry, 2005.

Normalized Difference Water Index

The NDWI is calculated based on the reflectance ratio between the Near-Infrared (NIR) and Short-Wave Infrared (SWIR) bands of Landsat 8 OLI/TIRS satellite imagery (Gao, 1996). The use of NIR (0.86 μm) and SWIR (1.24 μm) bands is effective in mapping the presence and extent of water bodies due to the distinct reflectance contrast between water surfaces and other land cover types. Moreover, the NDWI approach facilitates spatio-temporal analysis by accurately detecting changes in water bodies using Landsat 8 OLI/TIRS imagery (Santecchia et al., 2023). The Equation 2 used to calculate NDWI is as follows.

$$NDWI = \frac{(NIR - SWIR)}{(NIR + SWIR)} \quad (2)$$

where NIR represents the reflectance of near-infrared light, and $SWIR$ represents the reflectance of shortwave infrared light. Subsequently, the calculated index values at each point were classified into moisture level categories (Table 3).

Normalized Difference Built-Up Index

The NDBI is calculated based on the reflectance ratio between the Short-Wave Infrared (SWIR) band and the Near-Infrared (NIR) band from Landsat 8 OLI/TIRS satellite imagery. The wavelength range of the SWIR band (1.55 – 1.75 μm) and the NIR band (0.76 – 0.90 μm) enables the automated extraction of built-up areas from Landsat data. The index yields values ranging from -1 to +1, which indicate the density of built-ip surfaces (Zha et al., 2003).

Table 3. Classification of NDWI Values Based on Moisture Levels

NDWI Values (µm)	Level of Moisture
-0.43 – 0.1	Absent water
0.1 – 0.17	Low
0.17 – 0.27	Moderately low
0.27 – 0.37	Moderate
0.37 – 0.47	Moderately high
0.47 – 1.0	High

Source: Ji et al., 2009.

$$NDBI = \frac{(SWIR - NIR)}{(SWIR + NIR)} \quad (3)$$

where $SWIR$ represents the reflectance of shortwave infrared light, and NIR represents the reflectance of near-infrared light. Subsequently, the calculated index values at each point were classified into categories of built-up density levels (Table 4).

Table 4. Classificatioin of NDBI Values According to Building Density Levels

NDBI Values (µm)	Building Density
-1 - 0	Non-building
0 – 0.1	Rare
0.1 – 0.2	Medium
> 0.2	Dense

Source: Zha et al., 2003.

Land Cover

In this study, land cover analysis was conducted using supervised classification, which groups satellite image pixels based on spectral similarity in an iterative and automated manner. The method begins with the selection of training pixels for each land cover category. These pixels are then analyzed and identified based on the mean spectral distance and standard deviation of the clusters until convergence is achieved. This approach enables accurate and efficient multispectral classification for land cover mapping using Landsat 8 OLI/TIRS imagery (Phiri & Morgenroth, 2017).

Land Surface Temperature

The processing of LST data in this study was performed through several steps. First, the Digital Number (DN) values were converted into Spectral Radiance ($L\lambda$) following the approach using the the Equation 4 (Chander et al., 2009).

$$L\lambda = 0.0370588 \times \mathrm{DN} + 3.2 \quad (4)$$

where $L\lambda$ is the spectral radiance ($W \cdot m^{-2} \cdot sr^{-1} \cdot \mu m^{-1}$), and DN is the digital number of the thermal band.

The next step was converting Spectral Radiance to Brightness Temperature (Tb)using the radiometric calibration constants, according to Equation 5 (Chander et al., 2009).

$$\mathrm{Tb} = \frac{\mathrm{K2}}{In(\frac{K1}{L\lambda} + 1)} \quad (5)$$

where Tb is the brightness temperature in Kelvin, K1 and K2 are calibration constants provided in the Landsat matadata, and $L\lambda$ is the spectral radiance.

Finally, the Brightness Temperature was converted to LST using the method proposed by Equation 6 (Li et al., 2013).

$$\mathrm{LST} = \frac{\mathrm{Tb}}{[1 + \left(\frac{\lambda \mathrm{Tb}}{\alpha}\right) In\, \varepsilon} \quad (6)$$

where LST is the land surface temperature in Kelvin, λ is the effective wavelength of emitted radiance (for Landsat thermal bands), α is a constant (equal to $h \cdot c/\sigma$, where h is Planck's constant, c is the speed of light, and σ is Boltzmann's constant), and ε is the surface emissivity.

RESULT AND DISCUSSION

Normalized Difference Vegetation Index

The processing of NDVI data produced a map that illustrates vegetation density in South Jakarta from a spatial and temporal perspective (Figure 2). The NDVI map highlights the geographic variation of vegetation density across the region. Areas with high NDVI values (approaching +1) are associated with densely vegetated zones, such as urban parks or GOS, whereas highly built-up areas exhibit lower NDVI values (close to zero or negative).

The NDVI data were processed for four periods to facilitate a temporal analysis of vegetation cover change. The resulting maps clearly represent vegetation cover dynamics, allowing for year-to-year comparisons to assess the extent of land-use conversion (Kumar & Corbett, 2019).

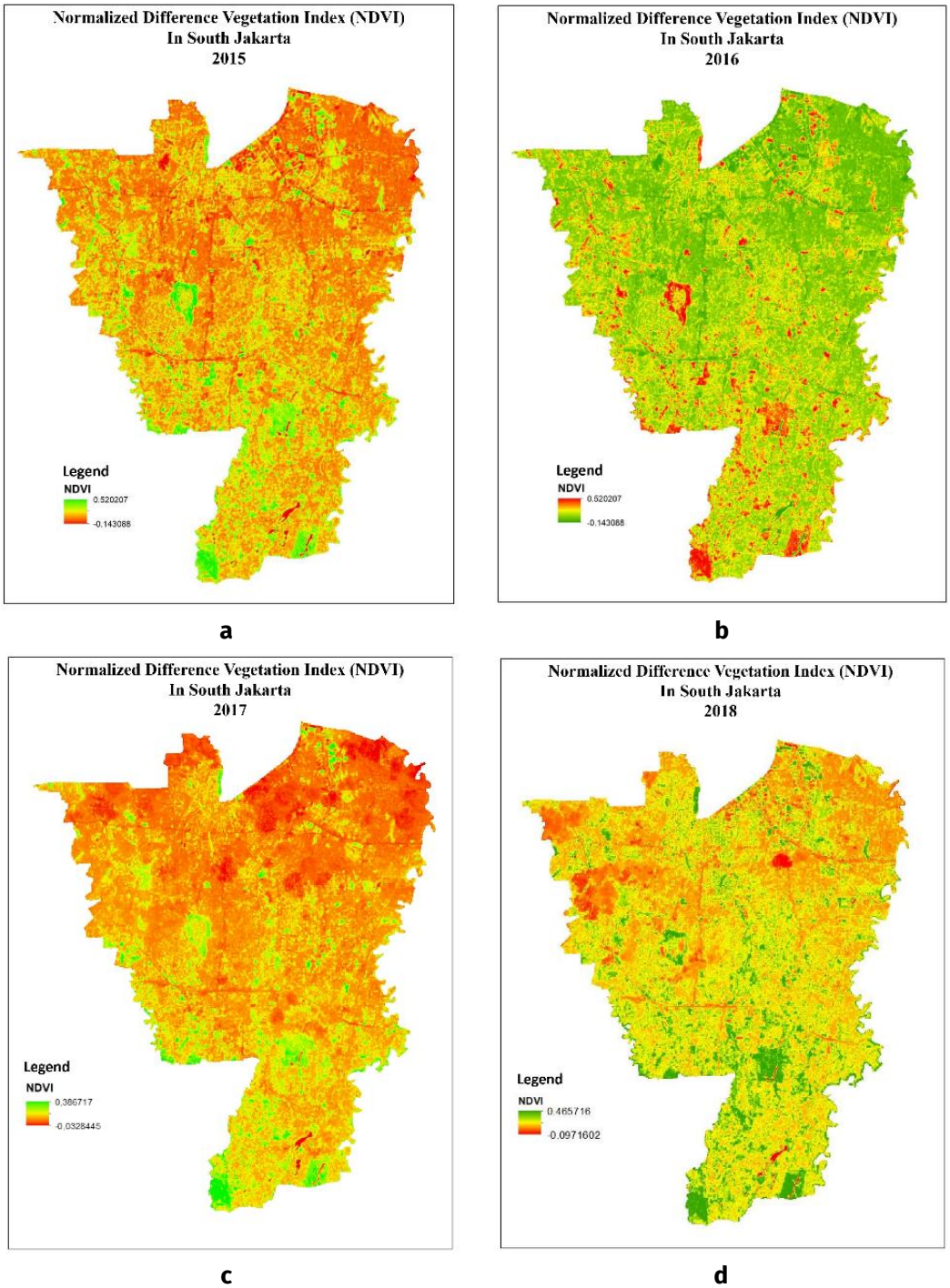

Figure 2. The Map of NDVI in a) 2015, b) 2016, c) 2017, and d) 2018

Based on the visualization of the NDVI map (Figure 2), the spatial distribution of vegetation density in South Jakarta demonstrates considerable variation from year to year. The green areas on the map represent regions with high vegetation cover, while red areas indicate non-vegetated or built-up land. Temporal analysis of NDVI values from 2015 to 2018 indicates fluctuations that reflect the dynamics of land conversion from vegetated to built-up areas. In 2015, the highest vegetation index was recorded at 0.50, which falls under the dense vegetation density category. However, in 2017, there was a significant decline in the vegetation index, with the highest value reaching only 0.30, categorized as rare. This decline in 2017 indicates a degradation of vegetation cover degradation due to urban development and the expansion of built-up or residential areas.

The findings of this study are consistent with those of Rachman et al. (2024), vegetation cover in Jakarta underwent a significant and continuous decline, primarily driven by the expansion of built-up areas. During the 2015-2020 period, the increase in built-up land was the most pronounced, whereas vegetation and water bodies experienced the highest levels of loss. The reduction in vegetation across Jakarta, including South Jakarta, was largely attributed to rapid population growth and the escalating demand for residential areas, with green spaces serving as the primary source of land conversion into built-up areas during this time.

Although the NDVI value in 2018 increased to 0.46, which falls into the good category, this condition likely reflects limited greening efforts, such as the development of small-scale GOS or localized vegetation planting. However, the long-term trend in South Jakarta, as demonstrated by Rachman et al. (2024), consistently indicates a decline in vegetation cover due to expansion of built-up areas. Therefore, the increase in NDVI in 2018 should be cautiously interpreted as a temporal fluctuation rather than evidence of sustainable vegetation recovery.

Furthermore, the highest NDVI value was still recorded in 2015, indicating that within the context of the correlation between NDVI and the UHI phenomenon, 2015 potentially experienced a lower UHI effect due to a high vegetation density of vegetation functioning as a surface temperature reducer (Voogt & Oke, 2003). These NDVI results are consistent with previous studies which stated that high NDVI values can reduce UHI intensity through the comparative vegetation effect (Furusawa et al., 2023). Therefore, NDVI fluctuations not only represent ecological changes but are also directly correlated with surface temperature dynamics, which constitute a key indicator in UHI studies.

Normalized Difference Water Index

The processing results of the NDWI in South Jakarta area provide a spatial and temporal representation of surface moisture distribution, which is directly related to the presence of water bodies and land humidity. In this study, NDWI maps are categorized into four periods: 2015, 2016, 2017, and 2018. Each map illustrates variations in surface moisture index that reflect the dynamics of water body availability and wetland areas over time.

High NDWI values represent the presence of water bodies or areas with high surface moisture, whereas low values indicate dry areas. Spatial and temporal analysis of NDWI is conducted because surface moisture index plays a role in influencing the thermal dynamics of urban areas, particularly in amplifying the intensity of the UHI phenomenon through increased surface temperatures. The NDWI maps for the South Jakarta area across the four periods are presented in Figure 3.

Based on visual interpretation of the NDWI maps (Figure 3), the distribution of surface moisture in South Jakarta exhibits temporal dynamics, as indicated by the gradient from blue (high values) to red (low values). In 2025, the highest NDWI value was recorded at 0.18, which falls under the moderately low category. In 2016, only a marginal decimal difference was observed, indicating a relatively consistent level of surface moisture during the first two years of observation. However, in 2017, the NDWI value dropped drastically to 0.07, classified as very low, suggesting an absence of surface wetness. This indicates a significant degradation of surface moisture in 2017. In 2018, the NDWI value rose again to 0.15, although it remained in the low category. The overall low NDWI values are closely associated with the limited presence of water bodies in South Jakarta, such as small and unevenly distributed lakes. Previous studies have emphasized that the availability and spatial distribution of water

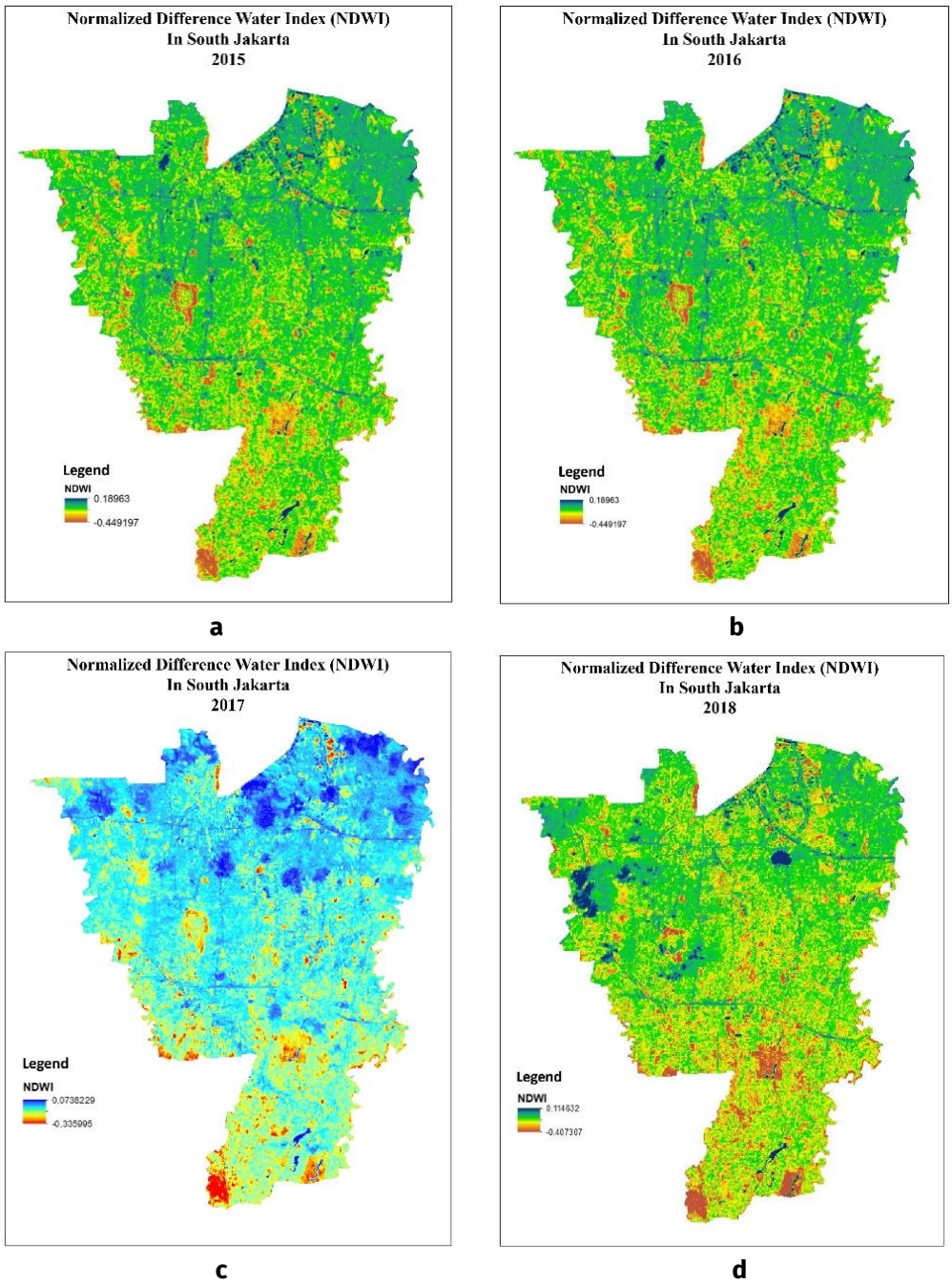

Figure 3. The Map of NDWI in a) 2015, b) 2016, c) 2017, and d) 2018

bodies are critical factors in determining surface moisture variability in urban areas (Gao, 1996). Other research further indicates that the presence of small and fragmented water bodies in highly urbanized regions often contributes to lower NDWI values (Chen et al., 2020).

Normalized Difference Built-Up Index

The processing of NDBI data from 2015 to 2018 produced maps (Figure 4) that illustrate building density levels based on five classification categories. Higher NDBI values reflect greater urban development intensity. This serves as an indicator (Zha et al., 2003).

Based on the visualization of the NDBI map (Figure 4), built-up areas are shown to dominate the South Jakarta region. This is indicated by the consistently high index values observed from 2015 to 2018. The color gradient from red (high building density) to blue (non-built-up areas), reflects the spatial distribution of development intensity. The highest NDBI values were recorded in 2015 and 2016, both reaching 0.23, indicating high building density.

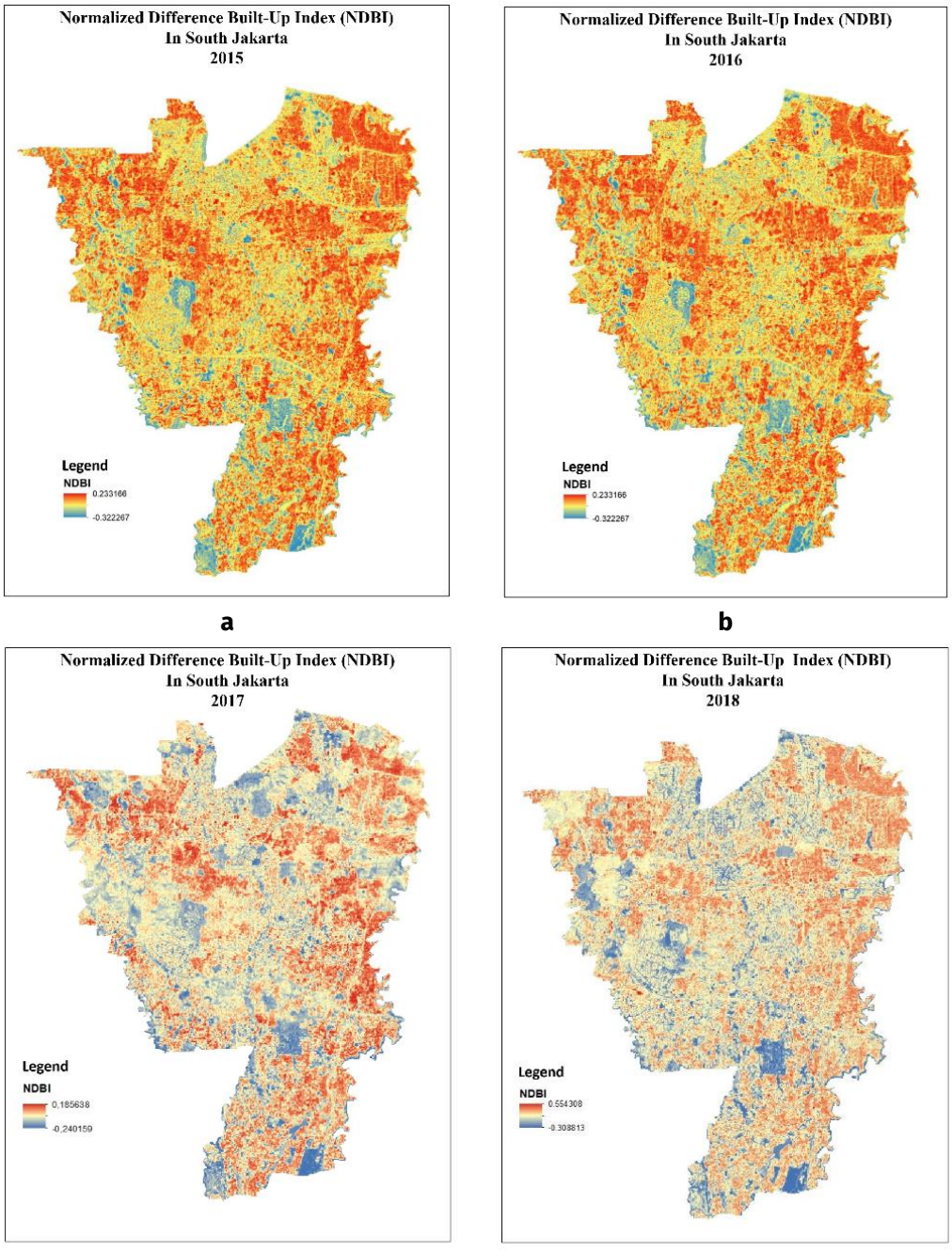

Figure 4. The Map of NDBI in a) 2015, b) 2016, c) 2017, and d) 2018

In 2017, the value declined to 0.18, before increasing sharply in 2018 to 0.55. These fluctuations suggest a dynamic and rapid physical expansion of the area, particularly in the residential and infrastructure sectors. This directly contributes to the intensification of the UHI phenomenon through increased heat emissions from built-up surfaces. Accordingly, the findings of this study align with prior research, which has demonstrated that the spatial distribution of built-up areas plays a critical role in intensifying the UHI phenomenon in metropolitan environments (Weng, 2001).

Land Cover

The result of land cover data processing using the Supervised Classification method from 2015 to 2018 produced maps that represent the spatial distribution of various land cover categories in South Jakarta (Figure 5). Based on the data analysis, land cover in South Jakarta was classified into four categories: built-up land (orange), vegetation (green), open land (brown),

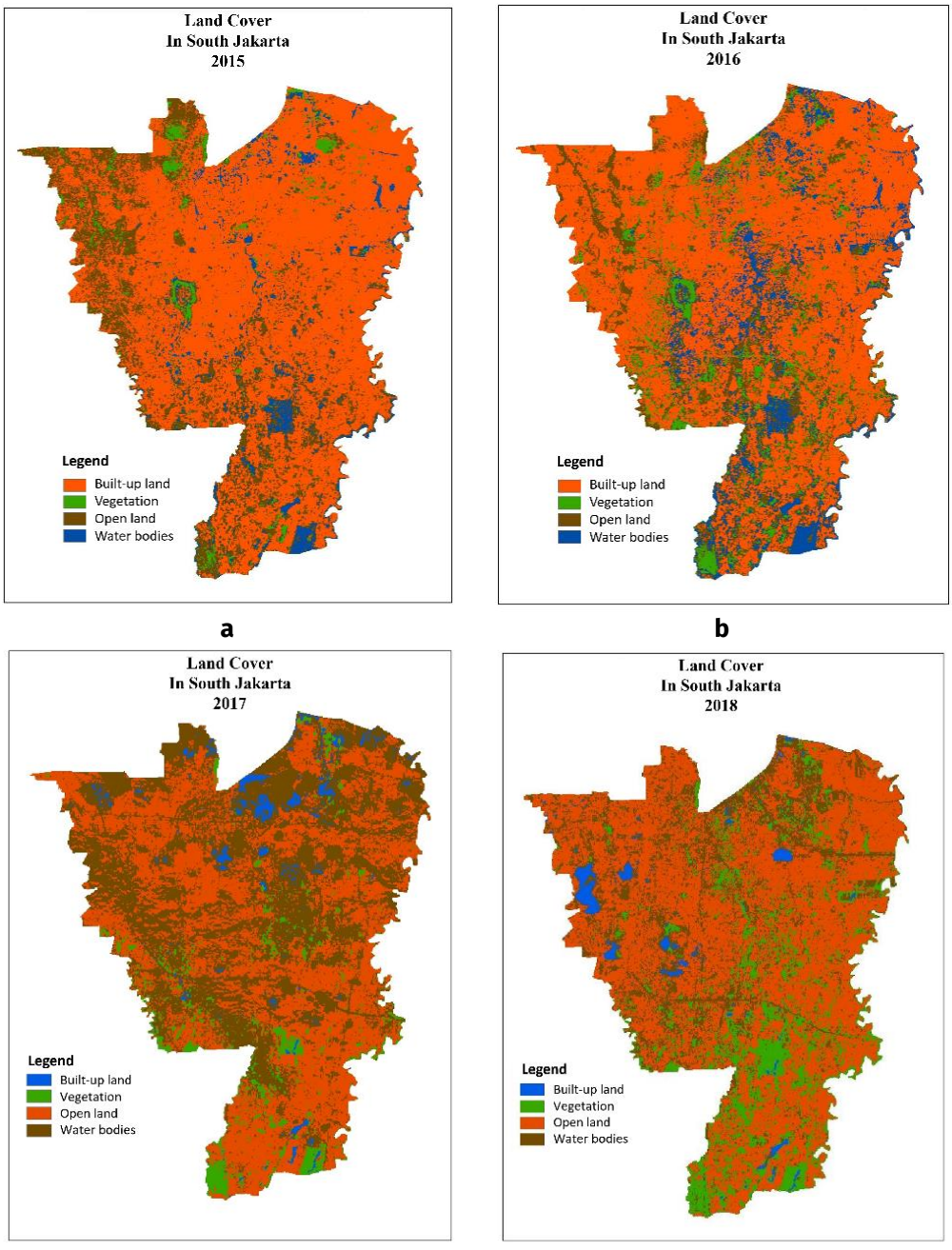

Figure 5. The Map of Land Cover in a) 2015, b) 2016, c) 2017, and d) 2018

and water bodies (blue). Each land cover category contributes differently to the intensity of the UHI phenomenon. For instance, built-up areas tend to contribute significantly to anthropogenic heat emissions, while vegetation and water bodies play a role in reducing surface temperatures and mitigating the UHI effect.

The generated land cover maps not only provide spatial information regarding the distribution of land cover categories but also serve as a foundation for integrated analyses with other indices such as NDVI and NDBI (Figure 5). In the context of urban thermal studies, land cover acts as a determining variable influencing the intensity of the UHI phenomenon, depending on the proportion and spatial distribution of each category. The spatial visualizations from these maps form the basis for examining the dynamics of land cover change and its temporal impact on the UHI phenomenon in South Jakarta.

Land Surface Temperature

The processed LST data are visualized in the form of maps (Figure 6), which display a gradient ranging from red to green. These maps

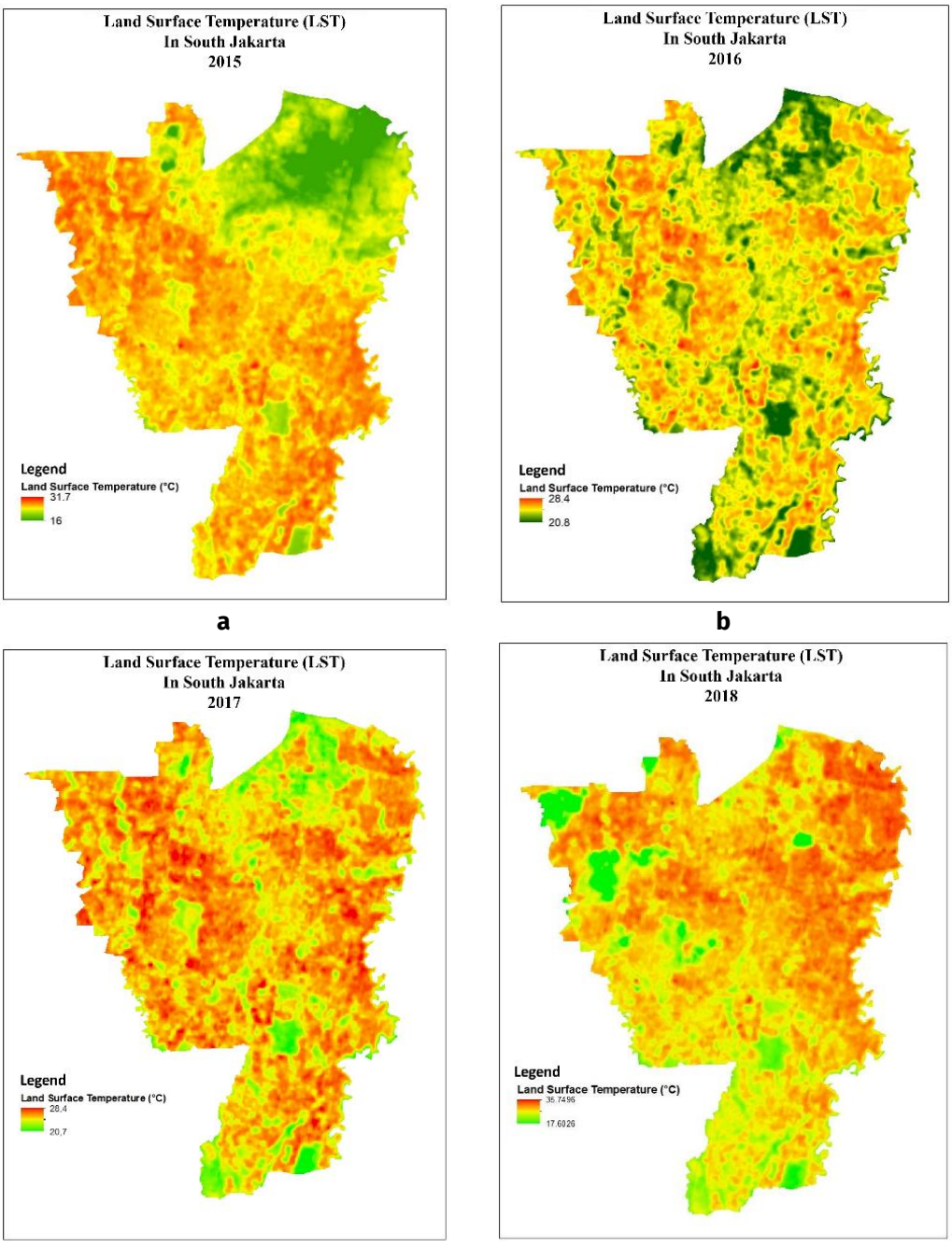

Figure 6. The Map of LST in a) 2015, b) 2016, c) 2017, and d) 2018

represent the spatial distribution of surface temperatures in the South Jakarta area. Red areas indicate zones with higher surface temperatures, while green areas reflect relatively lower temperatures. The LST mapping in this study was conducted temporally across four periods, allowing for the analysis of surface temperature changes over time.

The LST maps serves as a primary component in identifying the UHI phenomenon (Figure 6). This is because the map provides a concrete depiction of LST distribution that can be correlated with other variables such as NDVI, NDWI, NDBI, and land cover. This analysis is based on the principle that high surface temperatures generally show a positive show a positive correlation with the dominance of built-up areas and the limited presence of vegetation and water bodies (Weng et al., 2004). Thus, the LST map functions not only as a visual representation of surface temperatures but also as a fundamental basis for interpreting the spatial and temporal intensity and distribution of UHI in South Jakarta.

Assessing UHI Intensity in South Jakarta

Analysis of LST from 2015 to 2018 reveals that the UHI phenomenon in South Jakarta is dynamic and spatially uneven. The LST maps (Figure 6) show that areas with high surface temperatures, represented by red shades are predominantly located in built-up regions, particularly in the NDBI analysis, which recorded the highest index value in 2018 (0.55), indicating the dominance of built-up land cover and the limited presence of vegetation during that period.

In 2017, the spatial distribution of high surface temperatures in South Jakarta appeared the most uneven compared to other years. This disparity is likely associated with low surface moisture, as indicated by the lowest NDWI value recorded in 2017 (0.07). This value suggest minimal presence of water bodies and surface humidity, which in turn exacerbated local heating (Wu, et al., 2019). Conversely, in 2015, surface temperature conditions were relatively stable, consistent with the highest NDVI value (0.50), indicating a significant presence of vegetation functioning as a heat absorber (Santecchia et al., 2023).

In general, the spatial distribution of high surface temperatures depicted in the LST map demonstrates a strong correlation between land cover and other variables such as NDVI, NDWI, and NDBI (Figure 6). Areas with higher vegetation cover, as identified by green zones, consistently exhibit lower surface temperatures. In contrast, built-up and densely constructed areas tend to concentrate heat accumulation and intensify the effects of the UHI phenomenon in South Jakarta.

Dominant Variable on UHI Intensity

The correlation between spatial variables and LST, representing the UHI phenomenon, was analyzed using the Pearson Correlation Test. This analysis aimed to assess the degree of correlation between the independent variables (NDVI, NDWI, NDBI) and LST as the dependent variable for each observation year. The tabulated results show variations in the correlation strength among variables from 2015 to 2018, with interpretations based on Pearson's coefficient classification (Table 5).

In general, the NDBI variable exhibited the highest correlation values (0.55), consistently demonstrating a positive correlation with LST. This indicates that the expansion of built-up areas is closely associated with rising surface temperatures in urban environments. Meanwhile, both NDVI and NDWI tended to show negative correlations with LST, suggesting that areas with higher vegetation cover and surface moisture are capable of reducing UHI intensity (Weng et al., 2004). Based on statistical analysis, NDBI emerged as the dominant factor driving the increase in UHI intensity in South Jakarta during the study period.

The results of the yearly Pearson correlation test indicate that the influence of each variable on LST is dynamic. In 2015, NDVI showed the strongest negative correlation with LST, suggesting that vegetation played a significant role in lowering surface temperatures. This finding corresponds to the maximum NDVI value of 0.5 recorded in 2015, as illustrated in the NDVI map (Figure 2). In contrast, in 2016, NDBI exhibited the strongest positive correlation with LST, with an index value of 0.23, reflecting a high concentration of built-up areas. This trend highlights the dominance of anthropogenic heat resulting form intensified urban development. This finding is consistent with the study conducted by Weng (2001), which demonstrated that the increase in built-up area density is consistently associated with a rise in surface temperature and exacerbates the intensity of UHI in urban areas.

In 2017, all three variables (NDVI, NDWI, and NDBI) showed significant correlations with LST, indicating that spatial influences on surface temperature were more complex during that year. In contrast, in 2018, NDBI once again emerged as the variable with the strongest correlation to LST. this finding aligns with the interpretation of land cover maps, which revealed a notable increase in built-up areas and a significant decrease in vegetation cover. The relatively lower correlation values of NDVI and NDWI with LST (-0.208 and 0.180, respectively) suggest that in 2018, the influence of surface moisture and vegetation density on surface temperature was more limited compared to the impact of urban built-up areas. This is because the density of built-up areas plays a dominant role in elevating surface temperatures in urban environments, whereas the contributions of vegetation and water bodies are relatively limited, particularly in highly urbanized regions (Weng, 2001).

Table 5. Pearson Correlation Test Result for 2015 to 2018

	2015	LST	NDWI	NDVI	NDBI
2015	LST	Pearson Correlation	1	.029	-.067	.016
		Sig. (2-tailed)		.880	.723	.934
		N	30	30	30	30
	NDWI	Pearson Correlation	.029	1	-.988**	.788**
		Sig. (2-tailed)	.880		.000	.000
		N	30	30	30	30
	NDVI	Pearson Correlation	-.067	-.988**	1	-.853**
		Sig. (2-tailed)	.732	.000		.000
		N	30	30	30	30
	NDBI	Pearson Correlation	.016	.788**	-.853**	1
		Sig. (2-tailed)	.934	.000	.000	
		N	30	30	30	30
	2016	**LST**	**NDWI**	**NDVI**	**NDBI**
2016	LST	Pearson Correlation	1	.577**	-.620**	.705**
		Sig. (2-tailed)		.001	.000	.000
		N	30	30	30	30
	NDWI	Pearson Correlation	.577**	1	-.988**	.788**
		Sig. (2-tailed)	.001		.000	.000
		N	30	30	30	30
	NDVI	Pearson Correlation	-.620**	-.988**	1	-.853**
		Sig. (2-tailed)	.000	.000		.000
		N	30	30	30	30
	NDBI	Pearson Correlation	.705**	.788**	-.853**	1
		Sig. (2-tailed)	.000	.000	.000	
		N	30	30	30	30
	2017	**LST**	**NDWI**	**NDVI**	**NDBI**
2017	LST	Pearson Correlation	1	.630**	-.672**	.650**
		Sig. (2-tailed)		.000	.000	.000
		N	30	30	30	30
	NDWI	Pearson Correlation	.630**	1	-.988**	.610**
		Sig. (2-tailed)	.000		.000	.000
		N	30	30	30	30
	NDVI	Pearson Correlation	-.672**	-.988**	1	-.680**
		Sig. (2-tailed)	.000	.000		.000
		N	30	30	30	30
	NDBI	Pearson Correlation	.650**	.610**	-.680**	1
		Sig. (2-tailed)	.000	.000	.000	
		N	30	30	30	30
	2018	**LST**	**NDWI**	**NDVI**	**NDBI**
2018	LST	Pearson Correlation	1	-.208	.180	.473**
		Sig. (2-tailed)		.270	.340	.008
		N	30	30	30	30
	NDWI	Pearson Correlation	-.208	1	-.962**	.268
		Sig. (2-tailed)	.270		.000	153
		N	30	30	30	30
	NDVI	Pearson Correlation	.180	-.962**	1	-.461*
		Sig. (2-tailed)	.340	.000		.010
		N	30	30	30	30
	NDBI	Pearson Correlation	.473**	.268	-.461*	1
		Sig. (2-tailed)	.008	153	.010	
		N	30	30	30	30

**. Correlation is significant at the 0.01 level (2-tailed).

*. Correlation is significant at the 0.05 level (2-tailed).

The correlation patterns observed from 2015 to 2018 confirm that the influence of spatial variables on the intensity of the UHI phenomenon may vary each year, depending on

spatial conditions and land use dynamics. Nevertheless, NDVI and NDBI consistently emerge as the two most influential variables affecting surface temperature fluctuations in South Jakarta. This study is consistent with previous research demonstrating that the expansion of GOS significantly reduces LST, while the increase in built-up areas, as measured by the NDBI, shows a positive correlation with rising temperatures and the intensification of the UHI phenomenon in Jakarta (Rizki et al., 2024).

CONCLUSION

This study demonstrates that the UHI phenomenon in South Jakarta from 2015 to 2018 was dynamic and significantly influenced by both spatial and temporal variations in land cover change. Utilizing remote sensing technology and GIS, the intensity and distribution of UHI were identified through the analysis of NDVI, NDWI, NDBI indices, and land cover maps. The processed data revealed that the spatial distribution and intensity of UHI varied annually. Person correlation analysis indicated that NDVI and NDBI were the dominant variables influencing the UHI phenomenon. These findings highlight the importance of monitoring built-up areas and vegetation cover in controlling surface temperature increases in urban regions. This study emphasizes the necessity of adaptive and spatially informed urban planning to mitigate the impacts of UHI in metropolitan areas.

ACKNOWLEDGMENT

Our deepest gratitude is extended to all parties who have supported this research. Special appreciation is directed to the academic supervisors and lectures of the Urban Climatology course at the Department of Geography, Faculty of Mathematics and Natural Sciences, Universitas Indonesia, Dr. rer. nat. Eko Kusratmoko, M.S., and Faris Zulkarnain, S.Si., M.T., for their invaluable guidance and support. We also express our sincere thanks to the reviewers and editors of the Journal of Geographical Sciences and Education for their contributions in improving the quality of this manuscript.

REFERENCE

Chander, G., Markham, B. L., & Helder, D. L. (2009). Summary of Current Radiometric Calibration Coefficients for Landsat MSS, TM, ETM+, and EO-1 ALI Sensors. *Remote Sensing of Environment, 113*(5), 893-903. https://doi.org/10.1016/j.rse.2009.01.007

Chen, F., Chen, X., Van De Voorde, T., Roberts, D. A., Jiang, H., & Xu, W. (2020). Open Water Detection in Urban Environments using High Spatial Resolution Remote Sensing Imagery. *Remote Sensing of Environment, 242*, 111706. https://doi.org/10.1016/j.rse.2020.111706

Danniswari, D., Honjo, T., & Furuya, K. (2020). Land Cover Change Impacts on Land Surface Temperature in Jakarta and Its Satellite Cities. *IOP Conference Series Earth and Environmental Science, 501*(1),012031. https://doi.org/10.1088/1755-1315//501/1/012031

Deilami, K., Kamruzzaman, M., & Liu, Y. (2018). Urban Heat Island Effect: A Systematic Review of Spatio-Temporal Factors, Data, Methods, and Mitigation Measures. *International Journal of Applied Earth Observation and Geoinformation, 67*, 30-42. https://doi.org/10.1016/j.jag.2017.12.009

Department of Forestry. (2005). Pedoman Inventarisasi dan Identifikasi Lahan Kritis. Mangrove Directorate General of Land Realibility and Social Forestry. Jakarta

Eastman, J. R. (1997). IDRISI for Windows: User's Guide Version 2.0. Worcester, MA: Clark University.

Furusawa, T., Koera, T., Siburian, R., Wicaksono, A., Matsudaira, K., & Ishioka, Y. (2023). Time-Series Analysis of Satellite Imagery for Detecting Vegetation Cover Changes in Indonesia. *Scientific Reports, 13*(1), 8437. https://doi.org/10.1038/s41598-023-35330-1

Gao, B. C. (1996). NDWI-A Normalized Difference Water Index for Remote Sensing of Vegetation Liquid Water from Space. *Remote Sensing of Environment, 58*(3), 257-266. https://doi.org/10.1016/S0034-4257(96)00067-3

Imhoff, M. L., Zhang, P., Wolfe, R. E., & Bounoua, L. (2010). Remote Sensing of the Urban Heat Island Effect Across

Biomes in the Continental USA. *Remote Sensing of Environment, 114*(3), 504-513. https://doi.org/10.1016/j.rse.2009.10.008

Ji, L., Zhang, L., & Wylie, B. (2009). Analysis of Dynamic Thresholds for the Normalized Difference Water Index. *Photogrammetric Engineering & Remote Sensing, 75*(11), 1307-1317. https://doi.org/10.14358/PERS.75.11.1307

Kumar, P., & Corbett, L. J. (2019). Temporal Analysis of Urban Vegetation using NDVI in Rapidly Growing Megacities. *Urban Forestry & Urban Greening, 37*, 36-45. https://doi.org/10.1016/j.ufug.2018.12.008

Li, Z. L., Tang, B. H., Wu, H., Ren, H., Yan, G., Wan, Z., Trigo, I. F., & Sobrino, J. A. (2013). Satellite-Derived Land Surface Temperature: Current Status and Perspectives. *Remote Sensing of Environment, 131*, 14-37. https://doi.org/10.1016/j.rse.2012.12.008

Mukaka, M. (2012). Statistics Corner: A Guide to Appropriate use of Correlation Coefficient in Medical Research. *Malawi Medical Journal, 24*(3), 69-71.

Phiri, D., & Morgenroth, J. (2017). Developments in Landsat Land Cover Classification Methods: A Review. Remote Sensing, 9(9), 967. https://doi.org/10.3390/rs9090967

Rachman, F., Huang, J., Xue, X., Marfai, M. A. (2024). Insights from 30 Years of Land Use/Land Cover Transitions in Jakarta, Indonesia, Via Intensity Analysis. *Land, 13*(4), 545. https://doi.org/10.3390/land13040545

Rizki, A. R., Tumuyu, S. S., & Rushayati, S. B. (2024). The Impact of Urban Green Space on The Urban Heat Island Phenomenon – A Study Case in East Jakarta, Indonesia. *Geoplanning: Journal of Geomatics and Planning, 11*(1), 31-42. https://doi.org/10.14710/geoplanning.11.1.31-42

Santamouris, M. (2015). Regulating the Damaged Thermostat of the Cities—Status, Impacts and Mitigation Challenges. *Energy and Buildings. 91*, 43-556. https://doi.org/10.1016/j.enbuild.2015.01.027

Santecchia, G. S., Revollo Sarmiento, G. N., Genchi, S. A., Vitale, A. J., & Delrieux, C. A. (2023). Assessment of Landsat-8 and Sentinel-2 Water Indices: A Case Study in the Southwest of the Buenos Aires Province (Argentina). *Journal of Imaging, 9*(9), 186. https://doi.org/10.3390/jimaging9090186

Schwarz, N., Lautenbach, S., & Seppelt, R. (2011). Exploring Indications for Quantifying Surface Urban Heat Islands of European Cities with MODIS Land Surface Temperatures. *Remote Sensing of Environment, 115*(12), 3175-3186. https://doi.org/10.1016/j.rse.2011.07.003

USGS. (2023). Landsat 8 (OLI) Band Designations. Retrieved from: https://www.usgs.gov/core-science-systems/nli/landsat/landsat-8

Voogt, J. A., & Oke, T. R. (2003). Thermal Remote Sensing of Urban Climates. *Remote Sensing of Environment, 86*(3), 370-384. https://doi.org/10.1016/S0034-4257(03)00079-8

Wati, T., & Fatkhuroyan. (2017). Analisis Tingkat Kenyamanan di DKI Jakarta berdasarkan Indeks THI (Temperature Humidity Index). *Jurnal Ilmu Lingkungan, 15*(1). 57-63. https://doi.org/10.14710/jil.15.1.57-63

Weng, Q. (2001). A Remote Sensing-GIS Evaluation of Urban Expansion and Its Impact on Surface Temperature in the Zhujiang Delta, China. *International Journal of Remote Sensing, 22*(10), 1999-2014. https://doi.org/10.1080/713860788

Weng, Q., Lu, D., & Schubring, J. (2004). Estimation of Land Surface Temperature-Vegetation Abundance Relationship for Urban Heat Island Studies. *Remote Sensing of Environment, 89*(4), 467-483. https://doi.org/10.1016/j.rse.2003.11.005

Whidayanti, E., Handayanti, T., Supriatna., & Manessa, M. (2021). A Spatial Study of Mangrove Ecosystems for Abrasion Prevention using Remote Sensing Technology in the Coastal Area of Pandeglang Regency. *IOP Conference Series: Earth and Environmental Sciences, 771*(1), 012014. https://doi.org/10.1088/1755-1315/771/1/012014

Winarso, H., Hudalah, D., & Firman, T. (2015). Peri-Urban Transformation in the Jakarta

Metropolitan Area. *Habitat International*, *49*, 221-229. https://doi.org/10.1016/j.habitatint.2015.06.008

Wu, C., Li, J., Wang, C., Song, C., Chen, Y., Finka, M., & Rosa, D. L. (2019). Understanding the Relationship between Urban Blue Infrastructure and Land Surface Temperature. *Science of the Total Environment. 694*, 133742. https://doi.org/10.1016/j.scitotenv.2019.133742

Zha, Y., Gao, J., & Ni, S. (2003). Use of Normalized Difference Built-Up Index in Automatically Mapping Urban Areas from TM Imagery. *International Journal of Remote Sensing, 24*(3), 583-594. https://doi.org/10.1080/01431160304987

Zhou, D., Zhao, S., Liu, S., Zhang, L., & Zhu, C. (2014). Surface Urban Heat Island in China's 32 Major Cities: Spatial Patterns and Drivers. *Remote Sensing of Environment. 152*, 51-61. https://doi.org/10.1016/j.rse.2014.05.017

Zhou, D., Zhang, L., Li, D., Huang, D., & Zhu, C. (2016). Climate-Vegetation Control on the Diurnal and Seasonal Variations of Surface Urban Heat Islands in China. *Environmental Research Letters*, *11*(7), 074009. https://doi.org/10.1088/1748-9326/11/7/074009